RESEARCH ARTICLE

Associations of Alzheimer's Disease Pathology and Small Vessel Disease With Cerebral White Matter Degeneration: A Tract-Based MR Diffusion Imaging Study

Kaicheng Li,[1] Shuyue Wang,[1] Xiao Luo,[1] Qingze Zeng,[1] Xiaocao Liu,[1] Luwei Hong,[1] Jixuan Li,[1] Hui Hong,[1] Xiaopei Xu,[1] Yao Zhang,[1] Yeerfan Jiaerken,[1] Ruiting Zhang,[1] Linyun Xie,[1] Shan Xu,[1] Xinyi Zhang,[2] Yanxing Chen,[2] Zhirong Liu,[2] Minming Zhang,[1*] and Peiyu Huang[1*]

Background: White matter (WM) degeneration is a key feature of Alzheimer's disease (AD). However, the underlying mechanism remains unclear.
Purpose: To investigate how amyloid-β (Aβ), tau, and small vascular disease (SVD) jointly affect WM degeneration in subjects along AD continuum.
Study Type: Retrospective.
Subjects: 152 non-demented participants (age: 55.8–91.6, male/female: 66/86) from the ADNI database were included, classified into three groups using the A (Aβ)/T (tau)/N pathological scheme (Group 1: A−T−; Group 2: A+T−; Group 3: A+T+) based on positron emission tomography data.
Field Strength/Sequence: 3T; T1-weighted images, T2-weighted fluid-attenuated inversion recovery images, T2*-weighted images, diffusion-weighted spin-echo echo-planar imaging sequence (54 diffusion directions).
Assessment: Free-water diffusion model (generated parameters: free water, FW; tissue fractional anisotropy, FAt; tissue mean diffusivity, MDt); SVD total score; Neuropsychological tests.
Statistical Tests: Linear regression analysis was performed to investigate the independent contribution of AD (Aβ and tau) and SVD pathologies to diffusion parameters in each fiber tract, first in the entire population and then in each subgroup. We also investigated associations between diffusion parameters and cognitive functions. The level of statistical significance was set at $p < 0.05$ (false discovery rate corrected).
Results: In the entire population, we found that: 1) Increased FW was significantly associated with SVD and tau, while FAt and MDt were significantly associated with Aβ and tau; 2) The spatial pattern of fiber tracts related to a certain pathological marker is consistent with the known distribution of that pathology; 3) Subgroup analysis showed that Group 2 and 3 had more alterations of FAt and MDt associated with Aβ and tau; 4) Diffusion imaging indices showed significant associations with cognitive score in all domains except memory.
Data Conclusion: WM microstructural injury was associated with both AD and SVD pathologies, showing compartment-specific, tract-specific, and stage-specific WM patterns.
Evidence Level: 1
Technical Efficacy: Stage 3

J. MAGN. RESON. IMAGING 2023.

View this article online at wileyonlinelibrary.com. DOI: 10.1002/jmri.29022

Received Jun 4, 2023, Accepted for publication Sep 5, 2023.

*Address reprint requests to: P.H., Department of Radiology, The Second Affiliated Hospital, Zhejiang University School of Medicine, No. 88 Jiefang Road, Shangcheng District, Hangzhou 310009, China. E-mail: huangpy@zju.edu.cn, or M.Z., Department of Radiology, The Second Affiliated Hospital, Zhejiang University School of Medicine, No. 88 Jiefang Road, Shangcheng District, Hangzhou 310009, China. E-mail: zhangminming@zju.edu.cn
The first two authors contributed equally to this work.

From the [1]Department of Radiology, The Second Affiliated Hospital of Zhejiang University School of Medicine, Hangzhou, China; and [2]Department of Neurology, The Second Affiliated Hospital of Zhejiang University School of Medicine, Hangzhou, China

Additional supporting information may be found in the online version of this article

White matter (WM) degeneration is a key feature of Alzheimer's disease (AD).[1,2] Consistently reported in AD patients and subjects with mild cognitive impairment (MCI), WM degeneration is associated with cognitive decline in multiple domains.[2] While major AD histologic features including amyloid-β (Aβ) and tau deposition have been found related to the loss of axonal neurofilaments and myelin breakdowns,[3] other mechanisms may also participate in this process. Specifically, cerebral smalls vessel disease (SVD) is commonly concomitant within AD[4] and could contribute to WM degeneration through mechanisms such as hypoperfusion or blood–brain barrier disruption.[5] Understanding how these pathologic mechanisms jointly affect WM degeneration in AD may provide useful evidence for developing neuroprotective strategies.

Diffusion tensor imaging (DTI) has been widely applied to investigate WM alterations in AD.[6] While the results of increased mean diffusivity and decreased fractional anisotropy are relatively consistent in patients with AD or MCI,[1] their associations with different pathologies (Aβ or tau) are less congruent.[7–10] Some authors claimed that Aβ deposition is associated with WM alterations in AD predilection areas,[7] while others found that the loss of WM integrity was mainly associated with tau accumulation.[8] Furthermore, recent studies employing multicompartment diffusion models found that WM diffusivity changes in AD were mainly driven by increased non-parenchymal fluid. To disentangle the effects, several issues should be considered: first, AD and SVD pathologies can lead to various forms of WM alterations (eg, axon disruption, demyelination, and accumulation of non-parenchymal fluid).[3,9–11] Thus, multicompartment models should be adopted to detect different forms of WM changes. Second, AD and SVD pathologies are not uniformly distributed throughout the brain but display distinct spatial patterns. Specifically, Aβ deposition and SVD lesions are usually widespread,[12,13] while tauopathy tend to spread in a specific path, starting from the entorhinal cortex and spreading posteriorly to the posterior cingulate cortex.[14] Thus, tract-specific analysis is preferred over whole-brain analyses. Third, from the point of disease progression, AD can accumulate in a specific temporal-ordered pattern, with Aβ deposition at the earliest stages, followed by intracellular phosphorylated tau depositions.[15] During disease progression, WM degeneration may not be a linear process.[16] Therefore, observations in different AD stages are necessary. Currently, evidence from studies that simultaneously consider the above-mentioned factors are scarce.

Free-water (FW) imaging, a bi-tensor diffusion model, has been proposed to correct each voxel for contamination from freely diffusing extracellular water molecules.[17] The resulting fractional volume of the FW compartment estimates the extracellular water content, and the FW-corrected DTI metrics closely reflect changes in WM tissue.[17] FW model has been used in many neurological diseases, like AD, Parkinson's disease, and SVD, and has proven its sensitivity and effectiveness.[10,18] Interestingly, several studies applied FW model in AD research and found that increased extracellular water content is a dominating factor in AD-related diffusion changes.[9,10]

In this study, we aimed to investigate the associations between AD/SVD and WM degeneration considering multiple model compartments, specific fiber tracts, and disease stages. We hypothesized that SVD is associated with a widespread non-parenchymal fluid increase, while AD is associated with fiber tissue damage in the memory-related circuits and default mode network.

Materials and Methods

Data used in the current study were obtained from the Alzheimer's disease neuroimaging initiative (ADNI) database (http://www.adni-info.org). The primary goal of ADNI has been to identify serial magnetic resonance imaging (MRI), positron emission tomography (PET), biomarkers, and genetic characteristics that would support the early detection and tracking of AD and improve the clinical trial design. Written consents were obtained from all subjects at each site. The current study has been approved by the ADNI steering committee, and by the institutional review boards of the Second Affiliated Hospital of Zhejiang University School of Medicine.

Study Participants

For this study, we included subjects that had available T1-weighted structural images, T2-weighted fluid-attenuated inversion recovery images (FLAIR), T2*-weighted images, DTI data, Aβ PET data, and tau PET data, and had undergone comprehensive neuropsychological assessments.

Since this study was mainly focused on early disease stages, we only included non-demented subjects, which consisted of cognitively unimpaired (CU) and MCI subjects. The diagnoses were made by neurologists at admission. The CUs were defined as subjects who had a clinical dementia (CDR) rating scale score of 0, a mini-mental state examination (MMSE) between 24 and 30 (inclusive), Wechsler memory scale logical memory, WMS-LM, delay recall performance ≥9 for subjects with 16 or more years of education; ≥5 for subjects with 8–15 years of education; and ≥3 for 0–7 years of education; non-clinical depression (GDS-15 score <6) and absence of dementia. MCI was defined as subjects who had preserved activities of daily living, non-dementia, and objective cognitive impairments, as shown on the delayed recall test of the WMS-LM, as well as a CDR score of 0.5.[19] Exclusion criteria are listed below: 1) significant medical, neurological, and psychiatric illness; 2) head trauma history; 3) use of non-AD-related medication known to influence cerebral function; 4) clinical depression; 5) alcohol or drug abuse.

Finally, we included 152 non-demented subjects (75 subjects with Aβ-negative tau-negative (A−T−), 43 subjects with A+T−, and 34 subjects with A+T+) from the ADNI database (see flowchart in Fig. 1, and more detailed information in the Supplemental Material Data S1). The characteristics of the participants are summarized in Table 1.

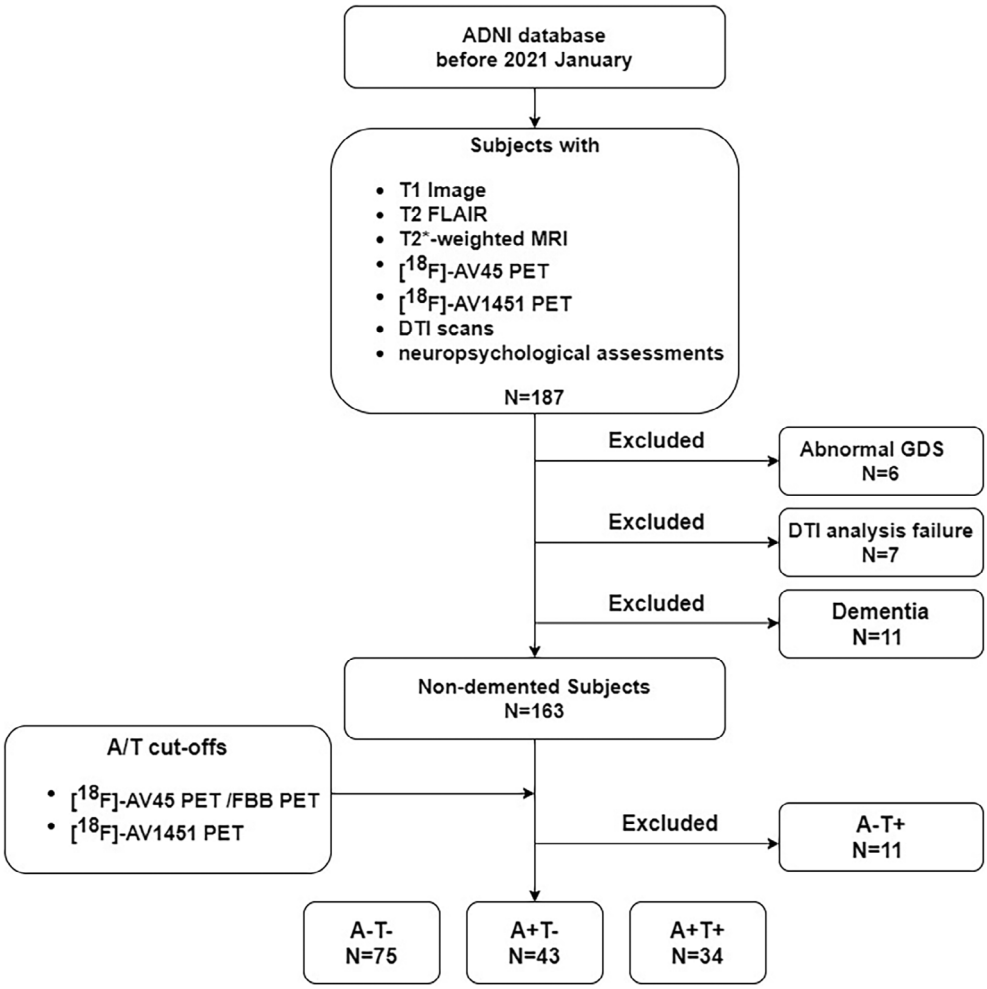

FIGURE 1: Flowchart of the subject inclusion. ADNI = the Alzheimer's disease neuroimaging initiative; T2 FLAIR = T2 fluid attenuated inversion recovery image; [^{18}F]-AV45 PET = ^{18}F-florbetapir positron emission tomography; FBB PET = ^{18}F-florbetaben positron emission tomography; [^{18}F]-AV1451 PET = ^{18}F-florTaucipir positron emission tomography; DTI = diffusion tensor imaging; GDS = geriatric depression scale; A = Aβ; T = tau; A−T− = normal Aβ and tau; A+T− = abnormal Aβ and normal tau; A+T + = abnormal Aβ and tau.

Neuropsychological Assessment

All subjects finished a set of neuropsychological tests, including the assessments of general mental status using the MMSE, CDR, and montreal cognitive assessment (MoCA), and cognitive function in different domains. We collected scores on memory (Auditory Verbal Learning Test, AVLT; WMS-LM, immediate and delayed memory), visuospatial function (clock-drawing test, CDT), processing speed (trail-making test part A, TMT-A), and executive function (trail-making test part B, TMT-B).

MRI and PET Acquisition

The ADNI imaging data were acquired from different centers using harmonized protocols and the full list of acquisition parameters can be seen on the ADNI scanning website (http://adni.loni.usc.edu/methods/mri-tool/mri-analysis/). All data were acquired using 3T scanners from three vendors (GE, Siemens, and Philips). Here, we list some representative imaging parameters.

The structural images were obtained based on a 3D Magnetization Prepared Rapid Acquisition Gradient Echo T1 weighted sequence, with the following parameters: voxel size = 1 × 1 × 1 mm^3; echo time (TE) = minimum; inversion time (TI) = 900 msec; repetition time (TR) = 2300 msec; 208 sagittal slices; within-plane field of view = 256 × 240 mm^2. The T2 FLAIR scans were obtained using an echo-planar imaging sequence: TE = 119 msec, TR = 4800 msec, TI = 1650 msec, 1.0 × 1.0 × 1.2 mm^3. Axial T2*-weighted MRI scans were obtained using a gradient echo sequence with the following parameters: TR = 650 msec, TE = 20 msec, Flip angle = 20°, number of slices =50, 1.1 × 0.9 × 1 mm^3. DTI images were obtained with a spin-echo echo planar imaging sequence using the following imaging parameters: TR = 12,400 msec, TE = minimum, 1.0 × 1.0 × 1.2 mm^3, *b* value =0, 1000 sec/mm^2, number of gradient directions = 54.

The amyloid PET was performed using two tracers, including the ^{18}F-florbetapir ([^{18}F]-AV45) and^{18}F-florbetaben (FBB), to maximize the sample size. Specifically, the [^{18}F]-AV45 PET in ADNI was acquired according to a standard dynamic 50–70 minutes protocol after the intravenous bolus injection of 370 ± 37 MBq of [^{18}F]-AV45. FBB PET in ADNI was acquired according to the below protocol: 300 MBq (8.1 mCi) ± 10%, 20 minutes (4 × 5 min frames) acquisition at 90–110 minutes post-injection.

TABLE 1. Demographic and Test Score Information

	Group 1 (A−T−)	Group 2 (A+T−)	Group 3 (A+T+)	All Subjects	*P*-Value
N	75	43	34	152	
Age (years)	71.86 ± 7.07	76.70 ± 8.18	75.72 ± 6.30	74.09 ± 7.54	0.001[a,b]
Female (%)	44/75	20/43	22/34	86/152	0.244
Education	16.29 ± 2.38	16.67 ± 2.58	16.50 ± 2.78	16.45 ± 2.52	0.726
GDS	1.03 ± 1.14	1.00 ± 1.13	1.32 ± 1.20	1.09 ± 1.15	0.392
Cognitive assessments					
MMSE	28.88 ± 1.21	28.09 ± 2.01	28.09 ± 1.58	28.48 ± 1.60	0.009[a,b]
CDR global	0.10 ± 0.20	0.14 ± 0.23	0.21 ± 0.25	0.13 ± 0.22	0.069
CDR sum	0.28 ± 0.58	0.49 ± 0.97	0.65 ± 0.94	0.42 ± 0.80	0.069
MoCA	25.68 ± 3.49	25.02 ± 3.43	23.15 ± 3.00	24.93 ± 3.49	0.002[b,c]
Memory function					
WMS-LM immediate	14.03 ± 3.94	13.81 ± 4.24	11.82 ± 4.99	13.47 ± 4.35	0.040[b,c]
WMS-LM delay	12.51 ± 4.26	12.70 ± 4.80	9.59 ± 5.98	11.91 ± 4.97	0.008[b,c]
AVLT sum of trials 1–5	45.68 ± 11.59	42.51 ± 12.21	37.88 ± 11.35	43.04 ± 12.04	0.006[b]
AVLT 30 minutes	8.31 ± 4.45	6.77 ± 4.41	4.44 ± 4.33	7.01 ± 4.64	<0.001[b,c]
Attention					
Log-transformed TMT-A	1.45 ± 0.13	1.51 ± 0.12	1.54 ± 0.21	1.48 ± 0.15	0.008[a,b]
Decision-making function					
Log-transformed TMT-B	1.83 ± 0.17	1.90 ± 0.19	1.92 ± 0.21	1.87 ± 0.19	0.039[b]
Language					
Category verbal fluency	21.63 ± 5.65	20.74 ± 6.04	18.35 ± 5.90	20.64 ± 5.92	0.027[b]
Visuospatial processing					
CDT	4.66 ± 0.64	4.56 ± 0.63	4.65 ± 0.54	4.63 ± 0.62	0.670
Pathological markers					
Global Aβ deposition	6.91 ± 8.83	62.33 ± 37.09	76.10 ± 36.15	38.06 ± 41.01	<0.001[a,b,c]

Tau PET was acquired using the ^{18}F-florTaucipir ([^{18}F]-AV1451). To be specific, the [^{18}F]-AV1451 PET in ADNI were acquired according to a standard dynamic 75–105 minutes protocol after the intravenous bolus injection of 370 ± 37 MBq of [^{18}F]-AV1451. More detailed information can be found on the ADNI website: http://adni.loni.usc.edu/methods/pet-analysis-method/pet-analysis/.

AD Pathological Markers

We used the Aβ and tau PET standardized uptake value ratio (SUVR) to reflect AD pathological burden (detailed information can be found in https://ida.loni.usc.edu/pages/access/studyData.jsp?categoryId=14).

Global Aβ values were determined for each subject by calculating a non-weighted average uptake across the frontal, anterior/posterior cingulate, lateral parietal, and lateral temporal lobes (segmented by Freesurfer, version 7.1.1, https://surfer.nmr.mgh.harvard.edu/) and dividing this average by the whole cerebellum uptake. We included both the [^{18}F]-AV45 and FBB PET data and then standardized them into the centiloid scale according to the method described previously. Global tau SUVR for each participant was computed by calculating median tau PET uptake in the entorhinal, amygdala, parahippocampal, fusiform, inferior temporal, and middle temporal regions (segmented by Freesurfer, version 7.1.1) normalized by the median tau PET uptake in the cerebellar crus gray matter.[20] The cutoffs to define Aβ and tau positivity were based on previous studies: SUVR ≥ 1.11 for [^{18}F]-AV45 PET, SUVR ≥ 1.08 for FBB SUVR, and SUVR ≥ 1.33 for [^{18}F]-AV1451.

SVD Markers Assessment

SVD markers were manually rated on structural MRI scans by three experienced radiologists, who were blinded to clinical information. The SVD scores were independently assessed by three neuroradiologist (KL, XL, and HPY) with 5, 5, and 10 years of experience. WM hyperintensity (WMH) were visually rated on FLAIR MRI according to the Fazekas scale.[21] Enlarged perivascular spaces (EPVS) were rated on T2-weighted MRI using a validated rating scale[22]; basal ganglia and centrum semiovale EPVS scores ranged from 0 to 4 according to EPVS count: 0 (none), 1 (1–10), 2 (11–20), 3 (21–40), and 4 (>40). Cerebral microbleeds (CMB) were assessed on susceptibility-weighted imaging following the microbleed anatomical rating scale.[23] Lacunes were identified using T1-weighted, T2-weighted, and FLAIR, following the standards for reporting vascular changes on neuroimaging guidelines.[24] Lacunes and CMB data were dichotomized separately as "present" (at least one lesion) or "absent" (no lesions).

In the current study, the total SVD score was computed using a 4-point system based on the presence or absence of four SVD markers, according to cutoffs defined by Staals et al.[25] Specifically, one point would be assigned to 1) periventricular WMWMH volume = 3 and/or deep WMH = 2 or 3 according to the Fazekas scale; 2) EPVS rating in basal ganglia ≥ 2; 3) presence of CMBs; 4) presence of lacunes. Inter-rater agreement was good (weighted kappa: 0.532).

Tractography

To reconstruct individual tracts, we used TRACULA (tracts constrained by underlying anatomy), a probabilistic automatic tracking

TABLE 1. Continued

	Group 1 (A−T−)	Group 2 (A+T−)	Group 3 (A+T+)	All Subjects	*P*-Value
TAU_METAROI	1.18 ± 0.09	1.22 ± 0.08	1.47 ± 0.16	1.26 ± 0.16	<0.001[b,c]
SVD total score	0.81 ± 0.91	1.09 ± 1.06	0.97 ± 1.03	0.93 ± 0.98	0.320

Data are presented as means ± standard deviations.
Aβ = beta-amyloid; Group 1 = non-demented with negative Aβ and tau; Group 2 = non-demented with positive Aβ and negative tau; Group 3 = non-demented with positive Aβ and tau; GDS = geriatric depression scale; MMSE = mini-mental state examination; CDR = clinical dementia rating; MoCA = montreal cognitive assessment; WMS-LM = Wechsler memory scale logical memory; AVLT = auditory verbal learning test; TMT = trail-making test; CDT = clock drawing test; SVD = small vessel disease.
[a]Group 1 vs. Group 2.
[b]Group 1 vs. Group 3.
[c]Group 2 vs. Group 3.

method based on Freesurfer (version 6.0, http://surfer.nmr.mgh.harvard.edu/fswiki) and FSL (version 6.0, https://fsl.fmrib.ox.ac.uk/fsldownloads).[26] Specifically, TRACULA utilizes the underlying anatomic pathways from the fiber tracts atlas of the training datasets and is capable of reconstructing 18 major WM tracts.[26] The workflow and technical details have been described in prior publications Specifically, A total of 18 WM bundles were reconstructed from each subject, including the corticospinal tract (CST), uncinate fasciculus (UF), inferior longitudinal fasciculus (ILF), anterior thalamic radiations (ATR), cingulum–cingulate gyrus bundle (Ccg), cingulum–angular bundle (Cab), superior longitudinal fasciculus–parietal branch (SLFp), superior longitudinal fasciculus–temporal branch (SLFt), corpus callosum–forceps major (FMajor), and corpus callosum–forceps minor (FMin). Except for the corpus callosum, all other pathways were reconstructed for the left (L) and right (R) hemispheres separately. Reconstructed tracts were visually inspected for each subject, and seven subjects with aberrant or truncated tracts were excluded.

FW Model

Diffusion imaging data were analyzed using an established FW imaging model.[17] This approach applies a regularization framework to fit a two-compartment model to diffusion-weighted images. The two compartments estimated in the FW model are 1) an anisotropic FW compartment, which quantifies the contribution of extracellular FW to the signal, and 2) a tissue compartment, modeled using a single diffusion tensor, which is corrected for FW.[17] Scalar measures, including FW-corrected tissue fractional anisotropy (FAt) and mean diffusivity (MDt), were calculated from the FW-corrected intracellular tissue compartment using FSL (version 6.0, https://fsl.fmrib.ox.ac.uk/fsldownloads).[27] Compared to conventional diffusion measures, FAt, and MDt could avoid water contamination and provide more robust estimation of WM microstructural integrity.[27] The model estimation was performed using a non-linear regularized minimization process implemented in MATLAB 2019b (https://www.mathworks.com/products/new_products/release2019b.html, MATHWORKS, Natick, MA, USA) as previously described.[17] The fractional volume of the FW compartment was estimated to produce an FW map. The FAt and MDt measures in each fiber tract reconstructed from TRACULA were calculated using the FSL *fslstats* tool.

Total Intracranial Volume (TIV) Calculation

Moreover, the TIV was calculated to correct the tract parameters for head size. We performed brain segmentation in each subject using the "recon-all" processing stream in FreeSurfer (version 6.0, https://surfer.nmr.mgh.harvard.edu/), which estimated the TIV.

Statistical Analyses

All statistical analyses were performed in SPSS 23 (https://www.ibm.com/support/pages/downloading-ibm-spss-statistics-23, IBM, Armonk, NY, USA). Associations between AD pathological markers (Aβ and tau), SVD markers (total SVD score), and tract-based diffusion parameters (FW, FAt, and MDt) were assessed using linear regression analyses within all subjects. The tract diffusion parameters were dependent variables and the AD\SVD markers were independent variable, with age, sex, education, and TIV as the covariates. Stepwise regressions were performed to identify factors that independently contributed to WM degeneration. False discovery rate (FDR, Benjamini–Hochberg method) correction was applied in analyses of each DTI parameter to reduce false positives. We then repeated these analyses in subgroups with different AD stages (A−T−, A+T−, and A+T+). Finally, associations between diffusion parameters and cognitive scores in each sub-domain were assessed within all subjects using linear regression analyses, with age, sex, and education as the covariates. The threshold for statistical significance was set as $P < 0.05$ (FDR-corrected). A visual abstract depicting the specific biomarkers and statistical analyses were provided (Fig. 2).

Results

Group 2 (A+T−) and 3 (A+T+) had significantly older age compared to Group 1 (A−T−). There was no significant

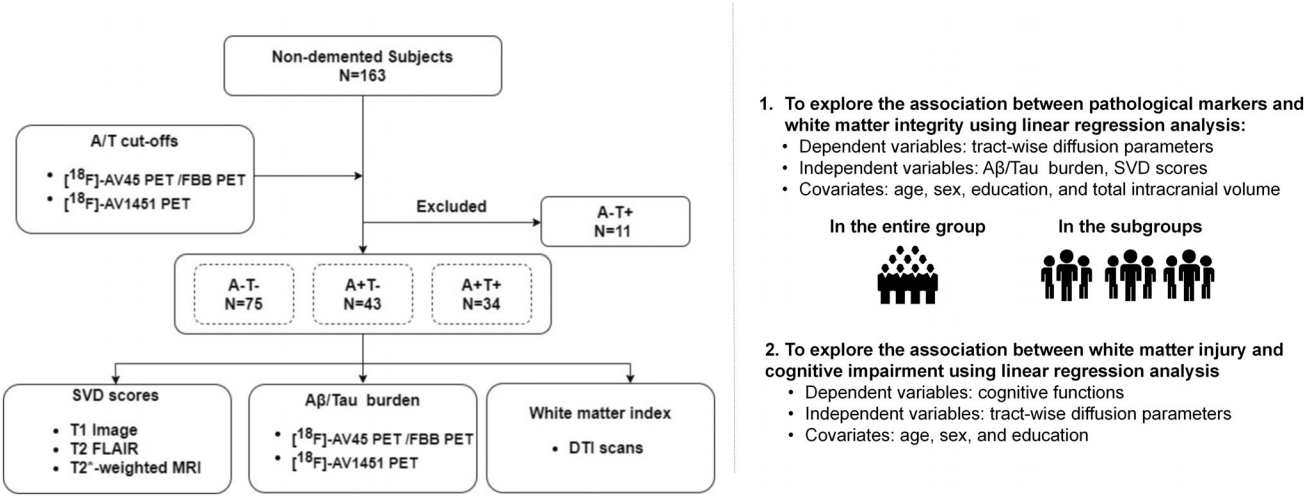

FIGURE 2: Visual abstract depicting the included biomarkers and statistical analyses. A = amyloid-β; T = tau; A−T− = normal Aβ and tau; A+T− = abnormal Aβ and normal tau; A+T+ = abnormal Aβ and tau; SVD = small vascular disease; T2 FLAIR = T2 fluid attenuated inversion recovery image; [^{18}F]-AV45 PET = ^{18}F-florbetapir positron emission tomography; FBB PET = ^{18}F-florbetaben positron emission tomography; [^{18}F]-AV1451 PET = ^{18}F-florTaucipir positron emission tomography; DTI = diffusion tensor imaging.

TABLE 2. An Overview of Associations Between Pathologies and WM Microstructural Changes

		Entire Population	Group 1	Group 2	Group 3
FW	Aβ				FMajor
	Tau	FMin, lh.Cab, rh.Cab	FMin, lh.Cab, rh.Cab, lh.UF, rh.UF		FMin
	SVD	lh.ATR, rh.ATR, lh.CST, rh.CST, lh.SLFp, rh.SLFp, lh.SLFt, rh. SLFt, lh.UF	lh.ATR, lh.SLFp, rh.SLFp	lh.ATR, rh.ATR, rh. CST	lh.ATR
FAt	Aβ	FMin, lh.ATR, rh.ATR, lh.Ccg, rh. Ccg, rh.CST, lh.SLFp, lh.SLFt, rh. SLFt		FMin, lh.CST, lh.SLFp, rh.SLFp, lh.SLFt, rh. SLFt	lh.Ccg, lh.SLFt
	Tau	rh.Cab, rh.ILF	lh.Cab, rh.Cab		FMin, lh.ATR, rh.ATR, rh. Ccg
	SVD				
MDt	Aβ	FMajor, FMin, lh.Ccg, rh.SLFp lh. SLFt		FMin	
	Tau	rh.Ccg	rh.SLFt		lh.Ccg, rh.Ccg, rh.CST
	SVD		rh.Cab		

FW = free-water; FAt = FW-corrected intracellular tissue fractional anisotropy; MDt = FW-corrected intracellular tissue mean diffusivity; rh = right hemispheric; lh = left hemispheric; CST = corticospinal tract; UF = uncinate fasciculus; ILF = inferior longitudinal fasciculus; ATR = anterior thalamic radiations; Ccg = cingulum−cingulate gyrus bundle; Cab = cingulum−angular bundle; SLFp = superior longitudinal fasciculus−parietal branch; SLFt = superior longitudinal fasciculus−temporal branch; Fmajor = corpus callosum−forceps major; Fmin = corpus callosum−forceps minor.

difference in sex ($P = 0.244$) and education ($P = 0.726$) among the three groups. Group 2 (A+T−) and 3 (A+T+) showed significantly worse cognition and higher load of AD pathologies compared to Group 1 (A−T−). Notably, there was no significant difference in SVD burden among the three groups ($P = 0.320$).

An Overview of Associations between Pathologies and WM Microstructural Changes

Due to the large amount of information, the full results of associations between pathologies (AD and SVD pathologies) and WM microstructural parameters (FW, FAt, and MDt) in 18 WM bundles were listed in Data S1 in the Supplemental Material. To help readers to gain an overview of the results, we listed the bundles showing significant associations with different pathological markers in different groups in Table 2.

Next, we will summarize all results from three aspects: 1) WM compartments: the pattern of associations between pathological markers and different WM compartments; 2) Fiber locations: the spatial pattern of fiber tracts associated with different pathological markers; and 3) AD stages: stage-specific patterns of WM changes associated with different pathologies. As these are descriptions from a high "pattern" level, please refer to Table 2 and Data S1 in the Supplemental Material if the readers want to look into a specific result.

WM Compartments (in the Entire Group)

Higher SVD burden was significantly associated with increased FW compartment in widespread regions (Fig. 3a, yellow color). Furthermore, Aβ was mainly associated with alterations in the tissue compartment (FAt and MDt). Higher Aβ was significantly associated with higher FAt, but associations with MDt depended on the specific fiber tracts (Fig. 3a, red color, Tables S1–S3 in the Supplemental Material). In contrast, associations with tau were quite restricted but involved both compartments (Fig. 3a, blue color). Specifically, higher tau was significantly associated with increased FW and decreased FAt in Cab.

Fiber Locations (in the Entire Group)

Almost all diffusion parameters in the frontoparietal tracts (CST, SLF, ATR, and UF) were significantly associated with both SVD and AD pathologies. Fiber tracts in the temporal

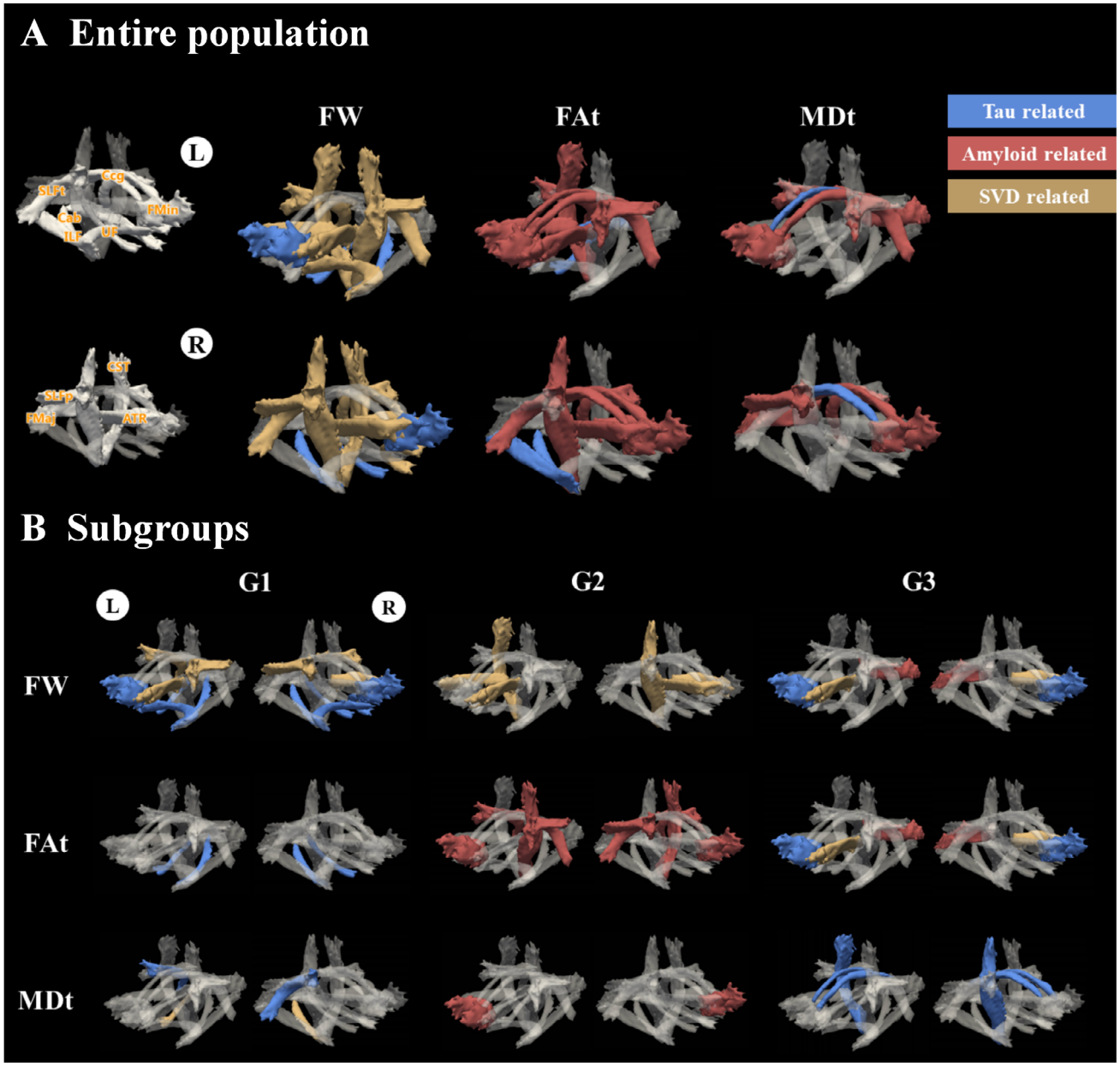

FIGURE 3: (a) Association between SVD\AD pathologies and WM alterations in the entire group, reflected by free water fraction and the tissue diffusivity measures (FAt and MDt). Significant associations between fiber tract alterations and different pathologies were color-coded, with yellow for SVD, blue for tau, and red for Aβ. (b) Association between SVD\AD pathologies and WM alterations in subgroups. Significant associations between fiber tract alterations and different pathologies were color-coded using the same scheme. SVD = small vessel disease; FW = free-water; FAt = FW-corrected fractional anisotropy; MDt = FW-corrected mean diffusivity; CST = corticospinal tract; UF = uncinate fasciculus; ILF = inferior longitudinal fasciculus; ATR = anterior thalamic radiations; Ccg = cingulum–cingulate gyrus bundle; Cab = cingulum–angular bundle; SLFp = superior longitudinal fasciculus–parietal branch; SLFt = superior longitudinal fasciculus–temporal branch; Fmajor = corpus callosum–forceps major; Fmin = corpus callosum–forceps minor; L = left; R = right; Aβ = beta-amyloid; T = tau; Group 1 = non-demented with negative Aβ and tau; Group 2 = non-demented with positive Aβ and negative tau; Group 3 = non-demented with positive Aβ and tau.

lobe (Cab and ILF) were significantly associated with tauopathy. Alterations in the occipital tract (Fmajor) were only significantly associated with Aβ, and alterations in Ccg and Fmin were significantly associated with both Aβ and tau. The detailed results are listed in Fig. 3a and Tables S1–S3 in the Supplemental Material.

Subgroup Analyses

In Group 1 (A−T−), SVD was significantly associated with higher FW in the ATR and SLFp, as well as lower MDt in the Cab. Tau was significantly associated with higher FW in the Cab, UF, and FMin, lower FAt in the Cab, and lower MDt in the SLFt.

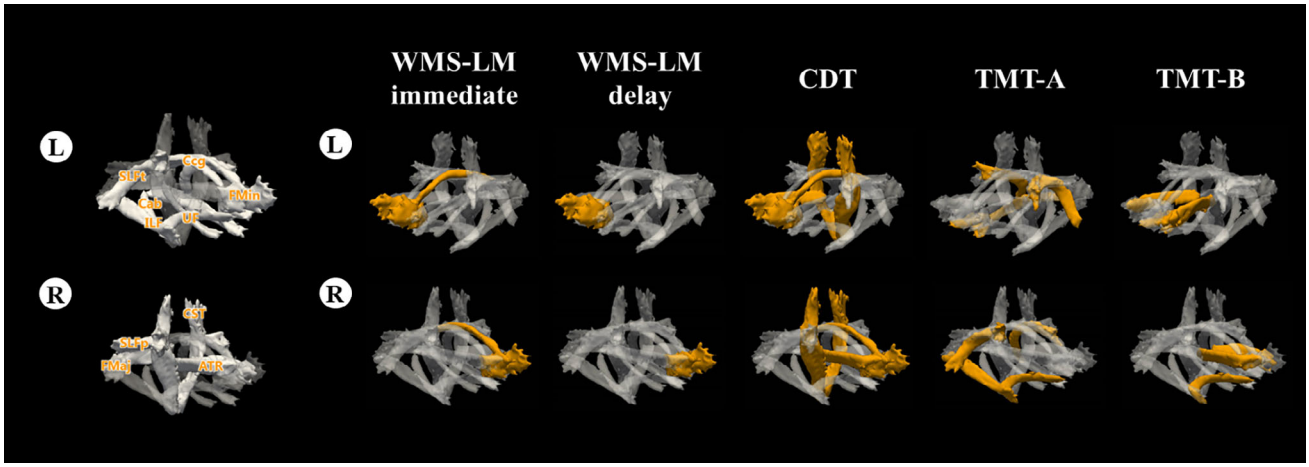

FIGURE 4: Associations between diffusion parameters and cognitive scores. WMS-LM = Wechsler memory scale logical memory; CDT = clock drawing test; TMT = trail-making test; CST = corticospinal tract; UF = uncinate fasciculus; ILF = inferior longitudinal fasciculus; ATR = anterior thalamic radiations; Ccg = cingulum–cingulate gyrus bundle; Cab = cingulum–angular bundle; SLFp = superior longitudinal fasciculus–parietal branch; SLFt = superior longitudinal fasciculus–temporal branch; Fmajor = corpus callosum–forceps major; Fmin = corpus callosum–forceps minor; L = left; R = right.

In Group 2 (A+T−), SVD was significantly associated with higher FW in the ATR and CST. Furthermore, Aβ was significantly associated with higher FAt in the SLFt, SLFp, CST, and FMin, as well as higher MDt in the FMin.

In Group 3 (A+T+), SVD was significantly associated with higher FW in the ATR. Moreover, Aβ was significantly associated with higher FW in the Fmajor and higher FAt in the SLFt and Ccg. Tau was significantly associated with higher FW in the FMin and higher FAt in the ATR, Fmin, and Ccg, as well as higher MDt in the Ccg and CST. Detailed information is shown in Fig. 3b and Tables S4–S6 in the Supplemental Material.

Associations between Diffusion Parameters and Cognition

In the entire group, there were significant associations between DTI parameters (FW, FAt, and MDt) and cognitive impairment in most cognitive domains except for language. 1) memory: worse WMS-LM immediate and delayed recall were associated with increased MDt in Fmin and left Ccg; 2) visuospatial function: worse CDT was associated with higher FW in bilateral CST, Fmin, and right ATR, and increased MDt in left Ccg; 3) processing speed: worse TMT-A was associated with increased FAt in bilateral SLFt, right ILF, and right UF; 4) executive function: worse TMT-B was associated with increased FW in bilateral ATR, and increased FAt in right UF. Detailed information is listed in Fig. 4 and Table S7 in the Supplemental Material.

Discussion

The current study investigated the associations between different pathologies (Aβ, tau, and SVD) and WM degeneration in subjects along the AD continuum. We found that Aβ, tau, and SVD were associated with distinct WM degeneration patterns specific to model compartments, fiber tracts, and disease stages. Furthermore, impairment in several cognitive domains (memory, visuospatial function, processing speed, and executive function) was associated with alterations in different fiber tracts.

According to previous work, AD pathologies were associated with WM damages.[28] We observed different trends for Aβ and tau. On one hand, we observed positive associations between Aβ and FAt, potentially indicating a compensation effect. This is partially consistent with previous studies, which found that a low Aβ burden was associated with decreased FA.[16,29] This is possibly due to the increased oligodendrocyte proliferation or remyelination of axons in early AD.[30] Nevertheless, we observed a negative association between FAt and cognition. Together, these results might indicate that the compensation is not sufficient for maintaining cognition. On the other hand, the associations with tau were limited in several fiber tracts but strong, most likely relating to changes in both compartments. In addition to disrupting axons, tau could cause severe fiber vacuolization and demyelination processes, which could also increase FW content.

SVD may act as the main contributor to increased FW in multiple regions, indicating elevated non-parenchymal fluid content. It might be related to a disrupted blood–brain barrier or glymphatic dysfunction due to vascular degeneration. Although the increased non-parenchymal fluid does not reflect tissue damage, it may facilitate WM degeneration. The result is consistent with recent studies investigating the FW content in SVD[31,32] and dementia cohorts,[2] suggesting that SVD, rather than AD pathology, may represent the dominating factor for increased FW.

The spatial pattern of fiber tracts related to a certain pathological marker is consistent with the known distribution of that pathology. The frontoparietal regions are targets of

both vascular degeneration and Aβ deposition.[12,13] Previous studies showed a higher WMH lesion burden in the frontoparietal lobes compared to the other lobes.[13] In addition, Aβ heavily deposits in the default mode network, which includes the medial frontal cortex.[12] Therefore, fiber tracts located in these areas suffered from mixed effects. In contrast, the temporal lobe is less susceptible to SVD but is a key region for tau accumulation, thus the Cab and ILF were mostly affected by tauopathy. Interestingly, while WMH is frequently seen in the posterior periventricular region, Aβ, but not SVD, was found to be associated with alterations in Fmajor. This confirmed the findings from two previous studies.[31,32]

Further subgroup analysis showed more FW changes in early stages, while more tissue compartment damage occurred in late stages. In Group 1 (A−T−), fiber degeneration was also associated with tauopathy. Tau is related to the aging process, and previous studies have found that in non-AD adults, tau accumulated during brain aging and was associated with the loss of WM integrity.[33,34] In Group 2 (A+T−), Aβ was the main pathology related to WM microstructural impairments, while the effect of SVD and tau were limited. In Group 3 (A+T+), the effect of tau was most prominent. This might be in line with the disease progression of AD. Notably, in all subgroups, SVD was associated with increased FW, and the effect was consistent in the ATR.

Cognitive impairment in all but the language domain was associated with altered WM diffusivity. For example, memory was associated with increased MDt in Fmin and left Ccg, which were targets of Aβ and tau, but not SVD. Therefore, we infer that SVD may contribute little to memory deficits through WM degeneration. The impairment in executive function was associated with changes in bilateral ATR and right UF. Notably, while the ATR has been consistently found associated with SVD,[35,36] our study showed that the UF was influenced by both AD and SVD. Therefore, both pathologies should be considered when examining the reasons of executive dysfunction.

Limitations

The sample sizes of the Group2 (A+T−) and 3 (A+T+) were relatively small, which is a major limitation of the present study. Further studies with larger sample sizes are needed to confirm the findings of this study. Additionally, the AD continuum was simulated by different disease stages. Longitudinal observations are needed to understand the association between disease evolution and WM degeneration.

Conclusion

We found that Aβ, tau, and SVD pathologies were associated with distinct WM degeneration patterns related to specific fiber tracts and disease stages in AD continuum.

Author Contributions

K.L., S.W., and P.H. designed the study. K.L. wrote the first draft of the manuscript. S.W. analyzed the MRI data and wrote the protocol. X.L. and Q.Z. collected clinical and MRI data. X.L., L.H., J.L., H.H., Z.Y., R.Z., L.X., S.X., X.Z., Y.C., Z.L., M.Z., and P.H. assisted with study execution and interpretation of findings. X.X., P.H., and J.Y. modified the expression and grammar thoroughly. All authors have contributed to and approved the final manuscript. All authors read and approved the final manuscript.

Funding Information

This study was supported by the National Natural Science Foundation of China (Grant Numbers: 82202090, 82271936, 82371907, 81901707, and 82001766), the China Postdoctoral Science Foundation (Grant Number: 2022M722751), Zhejiang Medical Health Science and Technology Program (Grant Number: 2023567844), and the Natural Science Foundation of Zhejiang Province (Grant Numbers: LSZ19H180001 and LQ20H180015).

Conflict of Interest

The authors declare no conflict of interest.

Ethics Approval Statement and Patient Consent Statement

All procedures performed in studies involving human participants were in accordance with the ethical standards of the institutional and national research committee and with the 1964 Helsinki declaration and its later amendments or comparable ethical standards. Written informed consent was obtained from all participants and authorized representatives, and the study partners before any protocol-specific procedures were carried out in the ADNI study. More details can be found at http://www.adni-info.org.

Data Availability Statement

The datasets analyzed in the current study are available on the ADNI website. More details in www.adni-info.org.

References

1. Mito R, Raffelt D, Dhollander T, et al. Fibre-specific white matter reductions in Alzheimer's disease and mild cognitive impairment. Brain 2018; 141(3):888-902.

2. Ji F, Pasternak O, Liu S, et al. Distinct white matter microstructural abnormalities and extracellular water increases relate to cognitive impairment in Alzheimer's disease with and without cerebrovascular disease. Alzheimers Res Ther 2017;9(1):63.

3. Nasrabady SE, Rizvi B, Goldman JE, Brickman AM. White matter changes in Alzheimer's disease: A focus on myelin and oligodendrocytes. Acta Neuropathol Commun 2018;6(1):22.

4. Azarpazhooh MR, Avan A, Cipriano LE, Munoz DG, Sposato LA, Hachinski V. Concomitant vascular and neurodegenerative pathologies double the risk of dementia. Alzheimers Dement 2018;14(2):148-156.
5. Joutel A, Chabriat H. Pathogenesis of white matter changes in cerebral small vessel diseases: Beyond vessel-intrinsic mechanisms. Clin Sci (Lond) 2017;131(8):635-651.
6. Mak E, Gabel S, Mirette H, et al. Structural neuroimaging in preclinical dementia: From microstructural deficits and grey matter atrophy to macroscale connectomic changes. Ageing Res Rev 2017;35:250-264.
7. Caballero MÁA, Song Z, Rubinski A, et al. Age-dependent amyloid deposition is associated with white matter alterations in cognitively normal adults during the adult life span. Alzheimers Dement 2020;16(4): 651-661.
8. Strain JF, Smith RX, Beaumont H, et al. Loss of white matter integrity reflects tau accumulation in Alzheimer disease defined regions. Neurology 2018;91(4):e313-e318.
9. Sepehrband F, Cabeen RP, Barisano G, et al. Nonparenchymal fluid is the source of increased mean diffusivity in preclinical Alzheimer's disease. Alzheimers Dement (Amst) 2019;11:348-354.
10. Finsterwalder S, Vlegels N, Gesierich B, et al. Small vessel disease more than Alzheimer's disease determines diffusion MRI alterations in memory clinic patients. Alzheimers Dement 2020;16(11):1504-1514.
11. Mitew S, Kirkcaldie MT, Halliday GM, Shepherd CE, Vickers JC, Dickson TC. Focal demyelination in Alzheimer's disease and transgenic mouse models. Acta Neuropathol 2010;119:567-577.
12. Mattsson NPS, Stomrud E, Vogel J, Hansson O. Staging β-amyloid pathology with amyloid positron emission tomography. JAMA Neurol 2019;76:1319-1329.
13. Wen W, Sachdev P. The topography of white matter hyperintensities on brain MRI in healthy 60- to 64-year-old individuals. Neuroimage 2004;22(1):144-154.
14. Braak H, Thal DR, Ghebremedhin E, Del Tredici K. Stages of the pathologic process in Alzheimer disease: Age categories from 1 to 100 years. J Neuropathol Exp Neurol 2011;70(11):960-969.
15. Jack CR Jr, Knopman DS, Jagust WJ, et al. Tracking pathophysiological processes in Alzheimer's disease: An updated hypothetical model of dynamic biomarkers. Lancet Neurol 2013;12(2):207-216.
16. Dong JW, Jelescu IO, Ades-Aron B, et al. Diffusion MRI biomarkers of white matter microstructure vary nonmonotonically with increasing cerebral amyloid deposition. Neurobiol Aging 2020;89:118-128.
17. Pasternak O, Sochen N, Gur Y, Intrator N, Assaf Y. Free water elimination and mapping from diffusion MRI. Magn Reson Med 2009;62(3): 717-730.
18. Duering M, Finsterwalder S, Baykara E, et al. Free water determines diffusion alterations and clinical status in cerebral small vessel disease. Alzheimers Dement 2018;14(6):764-774.
19. Bondi MWEE, Jak AJ, Clark LR, et al. Neuropsychological criteria for mild cognitive impairment improves diagnostic precision, biomarker associations, and progression rates. J Alzheimers Dis 2014;42:275-289.
20. Jack CR Jr, Wiste HJ, Weigand SD, et al. Defining imaging biomarker cut points for brain aging and Alzheimer's disease. Alzheimers Dement 2017;13(3):205-216.
21. Fazekas F, Chawluk JB, Alavi A, Hurtig HI, Zimmerman RA. MR signal abnormalities at 1.5 T in Alzheimer's dementia and normal aging. AJR Am J Roentgenol 1987;149(2):351-356.
22. Potter GM, Chappell FM, Morris Z, Wardlaw JM. Cerebral perivascular spaces visible on magnetic resonance imaging: Development of a qualitative rating scale and its observer reliability. Cerebrovasc Dis 2015; 39(3–4):224-231.
23. Gregoire SM, Chaudhary UJ, Brown MM, et al. The microbleed anatomical rating scale (MARS): Reliability of a tool to map brain microbleeds. Neurology 2009;73(21):1759-1766.
24. Wardlaw JM, Smith EE, Biessels GJ, et al. Neuroimaging standards for research into small vessel disease and its contribution to ageing and neurodegeneration. Lancet Neurol 2013;12(8):822-838.
25. Staals J, Makin SD, Doubal FN, Dennis MS, Wardlaw JM. Stroke subtype, vascular risk factors, and total MRI brain small-vessel disease burden. Neurology 2014;83(14):1228-1234.
26. Yendiki A, Panneck P, Srinivasan P, et al. Automated probabilistic reconstruction of white-matter pathways in health and disease using an atlas of the underlying anatomy. Front Neuroinform 2011;5:23.
27. Pasternak O, Kelly S, Sydnor VJ, Shenton ME. Advances in microstructural diffusion neuroimaging for psychiatric disorders. Neuroimage 2018;182:259-282.
28. Pichet Binette A, Theaud G, Rheault F, et al. Bundle-specific associations between white matter microstructure and Aβ and tau pathology in preclinical Alzheimer's disease. Elife 2021;10:10.
29. Collij LE, Ingala S, Top H, et al. White matter microstructure disruption in early stage amyloid pathology. Alzheimers Dement (Amst) 2021; 13(1):e12124.
30. Mathys H, Davila-Velderrain J, Peng Z, et al. Single-cell transcriptomic analysis of Alzheimer's disease. Nature 2019;570(7761):332-337.
31. Pålhaugen L, Sudre CH, Tecelao S, et al. Brain amyloid and vascular risk are related to distinct white matter hyperintensity patterns. J Cereb Blood Flow Metab 2021;41(5):1162-1174.
32. Weaver NA, Doeven T, Barkhof F, et al. Cerebral amyloid burden is associated with white matter hyperintensity location in specific posterior white matter regions. Neurobiol Aging 2019;84:225-234.
33. Schöll M, Lockhart SN, Schonhaut DR, et al. PET imaging of tau deposition in the aging human brain. Neuron 2016;89(5):971-982.
34. Gold BT, Zhu Z, Brown CA, et al. White matter integrity is associated with cerebrospinal fluid markers of Alzheimer's disease in normal adults. Neurobiol Aging 2014;35(10):2263-2271.
35. Duering M, Gesierich B, Seiler S, et al. Strategic white matter tracts for processing speed deficits in age-related small vessel disease. Neurology 2014;82(22):1946-1950.
36. Duering M, Zieren N, Hervé D, et al. Strategic role of frontal white matter tracts in vascular cognitive impairment: A voxel-based lesion-symptom mapping study in CADASIL. Brain 2011;134(8):2366-2375.